

THERMAL POSTBUCKLING OF SLENDER EXTENSIBLE PINNED-FIXED BAR UNDER NON-UNIFORM HEATING

Sumon Saha¹ and Abu Rayhan Md. Ali²

^{1,2}Department of Mechanical Engineering,
Bangladesh University of Engineering and Technology,
Dhaka-1000, Bangladesh

ABSTRACT

In this article, both thermal buckling and postbuckling of pinned-fixed bar subjected to transverse non-uniform temperature rise have been investigated. Based on the accurate geometrically nonlinear theory for Euler-Bernoulli beams, considering both linear and nonlinear strain-temperature relationships, governing equations for large deformations of the bar are derived. The two point boundary value problem for the nonlinear ordinary differential equations is solved effectively using the multisegment integration method. The numerical results show that both the critical buckling temperature and the postbuckled temperature of the bar are sensitively influenced by the slenderness ratio and nonlinear strain-temperature coefficient. It is also found that for uniform heating, the magnitude of the axially constrained force reaches a maximum value at the onset of the buckling state and then decreases as the temperature increases in the postbuckling regime. In addition, effects of non-uniform heating on the postbuckling behaviors are critically analyzed for the non-symmetric end condition.

Keywords: Thermal buckling, Multisegment method, Buckling temperature.

1. INTRODUCTION

The postbuckling of elastic slender beams has always been a fundamental topic in structural mechanics. Traditionally buckling is used as a failure criterion. However, nowadays flexible bars are being used as springs, linkages, robotic arms and satellite tethers. These structures are subjected to large variations in temperature during their life cycle. But compared with the study for the postbuckling of the beams subjected to mechanical loads, little was found in a search of literature on the thermal postbuckling of beams.

The investigations on thermal buckling and postbuckling of rods and beams are very necessary and important for the design of structures working in high temperature environments and of some thermal sensitive elastic elements. Because thermal elastic postbuckling of beams and rods are induced by the thermal bowing and thermal expansion, axial extension using geometric non-linear theory for extensible beams [1-9] must be considered in the analysis of this kind of problems. The postbuckling analysis of extensible beams or rods subjected to uniform and non-uniform heating has been carried out in the papers presented by El Naschie [1], Li [2-3], Li and Cheng [4], Li and Zhou [5] and Li et al. [6-7]. In order to obtain the secondary postbuckling equilibrium paths and configurations of the buckled beams or rods, a shooting method was employed. Vaz and Solano [8-9] developed a closed-form analytical solution via uncoupled elliptical integrals for the thermal postbuckling analysis of elastic slender rods with non-movable ends.

In this paper, the postbuckling behavior of a pinned-pinned beam presented by Li et al. [7] has been extended for the case of a pinned-fixed beam subjected to a temperature increase which is uniform in the longitudinal direction and non-uniform in the transverse direction of the beam. The material is assumed linear-elastic but its strain-temperature relationship is considered non-linear. Effects of both slenderness ratio and nonlinear strain-temperature coefficient on the postbuckling behaviors are qualitatively and quantitatively examined.

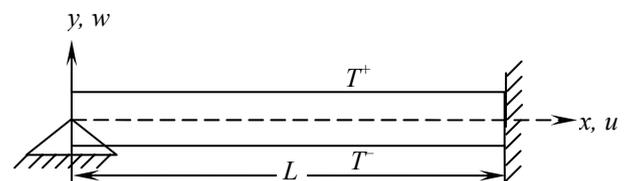


Fig 1: Geometry of immovable pinned-fixed bar subjected to non-uniform temperature rise

2. MATHEMATICAL FORMULATION

Let us consider an elastic bar of initial undeformed length L , rectangular cross-sections of constant width b and thickness h , and immovably one end pinned and other end fixed (Fig. 1). We assume that the bar is subjected to temperature rising T^+ at the top surface and T^- at the bottom from its undeformed state and also that the temperature distribution along the thickness is linearly changed. So the non-uniform static temperature

rise field T produces deformation of the bar from its stress free state and can be expressed as follows:

$$T = T_m + T_d y \quad \left(-\frac{h}{2} \leq y \leq \frac{h}{2} \right) \quad (1)$$

where $T_m = (T^+ + T^-) / 2$ is a mean value of the top and bottom temperature rises, and $T_d = T^+ - T^-$ is the difference between them. Herein, we assume that $T_d \geq 0$. By accurately taking into account the axial extension and the curvature of the deformed axial line, we examine the geometrically non-linear response of the bar, and give the non-dimensional governing equations of the problem as follows [10]:

$$\frac{dS}{d\xi} = \mu \quad \frac{dU}{d\xi} = \mu \cos \theta - 1 \quad \frac{dW}{d\xi} = \mu \sin \theta \quad (2)$$

$$\frac{d\theta}{d\xi} = -m - \frac{\tau_d}{2\sqrt{3}\lambda} \quad \frac{dm}{d\xi} = \mu [-P_h \sin \theta + P_v \cos \theta] \quad (3)$$

$$\frac{dP_h}{d\xi} = 0 \quad \frac{dP_v}{d\xi} = 0 \quad \frac{d\tau_m}{d\xi} = 0 \quad (4)$$

$$\mu = 1 + \frac{1}{\lambda^2} \left(\tau_m + \gamma \frac{\tau_m^2}{\lambda^2} - P_h \cos \theta - P_v \sin \theta \right) \quad (5)$$

The dimensionless quantities in the above equations are defined as follows:

$$(\xi, S, U, W) = (x, s, u, w) / L \quad \lambda = L \sqrt{(A/I)} \quad (6)$$

$$(\tau_m, \tau_d) = \lambda^2 \alpha (T_m, T_d) \quad \gamma = L_o / E \quad (7)$$

$$(P_h, P_v) = L^2 (H, V) / EI \quad m = LM / EI \quad (8)$$

The boundary conditions of a bar with pinned-fixed ends can be written in dimensionless forms as follows:

$$S(0) = U(0) = W(0) = m(0) = 0 \quad (9)$$

$$U(1) = W(1) = \theta(1) = 0 \quad (10)$$

In addition to the boundary conditions, a normalization relationship is imposed for the pinned-fixed bar as $\theta(0) = \theta_o$, where θ_o is the end rotational angle of the pinned end. Then, for a specified non-vanishing value of deformation control parameter θ_o and transverse temperature change parameter τ_d , we can determine a thermal postbuckling solution $(S, U, W, \theta, m, P_h, P_v)$ together with the value of the non-dimensional mean temperature rise τ_m for a specific buckling mode shape through Eqs. (1)-(3).

3. MULTISEGMENT INTEGRATION METHOD

It is difficult to obtain analytical solutions to the boundary value problems. For the symmetric buckling response of a uniformly heated rod with pinned-pinned ends, an elliptic integral solution was obtained [8]. The use of elliptic integrals as a possible method of solution to the titled problem is precluded because the boundary conditions about θ are not symmetric. Thus, the nonlinear governing equations of thermal postbuckling analysis have been solved here by using the method of multisegment integration developed by Kalnins and Lestingi [11]. For convenience, Eqs. (1)-(3) can be written in standard form as

$$\frac{d\bar{Y}}{d\xi} = F(\xi, \bar{Y}) \quad (11)$$

where

$$\bar{Y}(\xi) = \begin{bmatrix} y_1 \\ y_2 \\ y_3 \\ y_4 \\ y_5 \\ y_6 \\ y_7 \\ y_8 \end{bmatrix} = \begin{bmatrix} S \\ U \\ W \\ \theta \\ m \\ P_h \\ P_v \\ \tau_m \end{bmatrix} \quad F = \begin{bmatrix} \mu \\ \mu \cos y_4 - 1 \\ \mu \sin y_4 \\ -y_5 - \frac{\tau_d}{2\sqrt{3}\lambda} \\ \mu(-y_6 \sin y_4 + y_7 \cos y_4) \\ 0 \\ 0 \\ 0 \end{bmatrix}$$

$$\mu = 1 + \frac{1}{\lambda^2} \left(y_8 + \gamma \frac{y_8^2}{\lambda^2} - y_6 \cos y_4 - y_7 \sin y_4 \right)$$

The boundary conditions Eqs.(9)-(10) can be rearranged as follows:

$$A\bar{Y}(0) + B\bar{Y}(1) = C \quad (12)$$

where

$$A = \begin{bmatrix} 1 & 0 & 0 & 0 & 0 & 0 & 0 & 0 \\ 0 & 1 & 0 & 0 & 0 & 0 & 0 & 0 \\ 0 & 0 & 1 & 0 & 0 & 0 & 0 & 0 \\ 0 & 0 & 0 & 1 & 0 & 0 & 0 & 0 \\ 0 & 0 & 0 & 0 & 1 & 0 & 0 & 0 \\ 0 & 0 & 0 & 0 & 0 & 1 & 0 & 0 \\ 0 & 0 & 0 & 0 & 0 & 0 & 1 & 0 \\ 0 & 0 & 0 & 0 & 0 & 0 & 0 & 1 \end{bmatrix} \quad B = \begin{bmatrix} 0 & 0 & 0 & 0 & 0 & 0 & 0 & 0 \\ 0 & 0 & 0 & 0 & 0 & 0 & 0 & 0 \\ 0 & 0 & 0 & 0 & 0 & 0 & 0 & 0 \\ 0 & 0 & 0 & 0 & 0 & 0 & 0 & 0 \\ 0 & 0 & 0 & 0 & 0 & 0 & 0 & 0 \\ 0 & 1 & 0 & 0 & 0 & 0 & 0 & 0 \\ 0 & 0 & 1 & 0 & 0 & 0 & 0 & 0 \\ 0 & 0 & 0 & 1 & 0 & 0 & 0 & 0 \end{bmatrix} \quad C = \begin{bmatrix} 0 \\ 0 \\ 0 \\ 0 \\ 0 \\ \theta_o \\ 0 \\ 0 \end{bmatrix}$$

Now solutions of Eq. (11) by the method of multisegment integration in the interval $\xi_l \geq \xi \geq \xi_{M+1}$, where ξ_l corresponds to pinned end point ($\xi = 0$) and ξ_{M+1} corresponds to fixed end point ($\xi = 1$) of the bar at which the boundary condition, Eq. (12) is applicable, consists of the following steps:

(1) Division of the given interval of ξ into M sufficiently small segments so that the length of each segment is less than the critical meridional length as defined by Sepetoski et al. [12].

(2) Integration of Eq. (11) over each of the M segments as an initial value problem. The initial values used for starting in each segment are arbitrary.

(3) Integration of eight additional initial-value problems in each segment for which the variables are the derivatives of the eight fundamental variables $S, U, W, \theta, m, P_h, P_v$ and τ_m with respect to each of their initial values. The necessary equations for these integrations may be derived by differentiating Eqs. (1)-(3) with respect to the initial values of each of the eight fundamental variables. The initial values for these eight initial value problems are the columns of a 8×8 unit matrix.

(1) Solution of a system of M matrix equations, which ensures continuity of the variables at the end points of the segments.

(2) Repetition of steps (2), (3) and (4) until the conditions of continuity of the variables at the end of the segments are satisfied. In each pass the improved values of the variables obtained in step (4) are used as their initial values in step (2). The convergence of the solution is achieved when the improved values of the variables at the initial point of the bar segment as obtained from step (4) match with the trial initial values for the initial value integration of Eq. (11).

The derivation of the necessary differential equations for carrying out the integration of eight additional

initial-value problems and more details about the multisegment integration method are discussed in Ref. [10].

4. RESULTS AND DISCUSSIONS

The numerical solution is implemented through a computational program developed in the mathematical software Mathcad 14 [13] and a parametric study is carried out with the purpose of analyzing the results for bar slenderness ratios $\lambda = 50, 100, 150$ and 200 and for dimensionless transverse temperature rise, $\tau_d = 0, 10, 20$ and 30 .

4.1 Critical Temperature for Thermal Buckling

From the physical meaning of the problem, the onset of buckling is determined by the linearized problem of Eq. (11) and can be arrived at by the limit as θ_o goes to zero in Eqs. (12). The minimum of τ_m at which a nontrivial solution of the linearized problem exists is called critical nondimensional temperature defined by $\tau_m = \tau_{cr}$. Numerical results of the nondimensional critical temperature rise τ_{cr} corresponding to the magnitude of λ and γ are listed in Table 1. The results presented for $\gamma = 0$ and $\gamma = -5$ (metallic materials) are corresponded to materials with linear and nonlinear strain-temperature relationships respectively.

Table 1: Nondimensional critical temperature rise τ_{cr} at various slenderness ratios

Slenderness ratio λ	Nonlinear thermal strain coefficient	
	$\gamma = 0$	$\gamma = -5$
50	20.19	21.08
100	20.19	20.39
150	20.19	20.28
200	20.19	20.24

It is found that both the geometric parameter λ and the physical parameter γ have effects on τ_{cr} . For Eq. (4), we can see that the axial stretching is related to parameter γ or λ . Obviously, only for $\gamma = 0$, τ_{cr} is independent of the geometric parameter λ , the slenderness ratio of the bar. But for $\gamma \neq 0$, the value of τ_{cr} decreases with the increment of the value of λ and increases with the change of the value of γ .

4.2 Validation of the results

In order to verify the accuracy of the numerical results and the validity of the present mathematical model developed throughout the present study, comparisons with the previously published results have been carried out. Figure 2 shows the post-buckling deformed configuration presented by Li et al. [6] and the present study. In this figure, the solid line corresponds to the results of the present works while the legend marks correspond to those of Li et al. [6]. The overall tendency of the present results is completely the same as that of calculated by Li et al. [6].

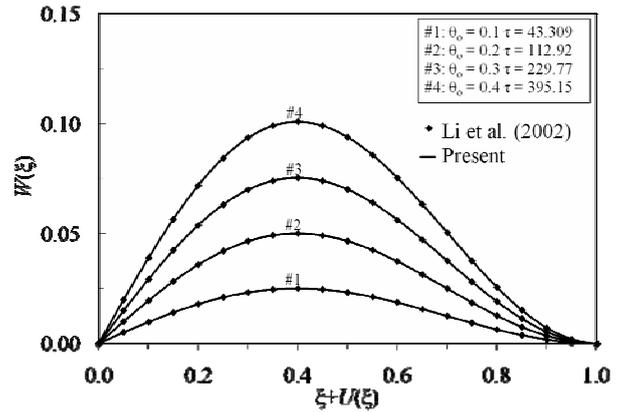


Fig 2: Comparison of Thermal Post-Buckling Deformed Configurations of a Pinned-Fixed Ended Rod for the Results Obtained in the Present Work and Those Obtained by Li et al. [6] at $\lambda = 120$ and $\gamma = 0$

4.3 Characteristics of postbuckling behavior

For a specific parameter θ_o or τ_m , the thermal postbuckled configurations of the bar, $W(\xi)$ is obtained as shown in Fig. 3. From these figure, it can be seen that each curve attains its maximum amplitude at $\xi = 0.4$ approximately, due to non-symmetric end condition.

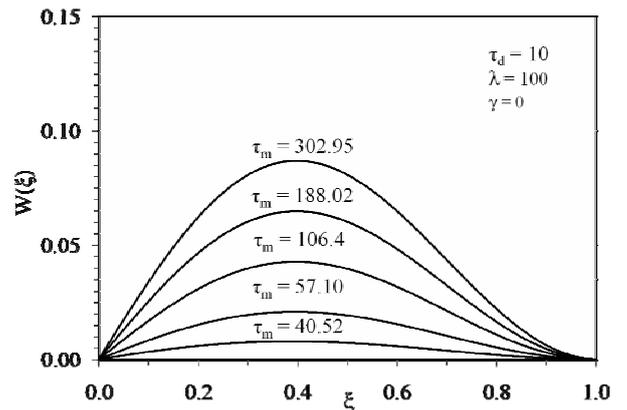


Fig 3: Thermal Post-Buckling Configuration of Bar with $\tau_d = 10, \lambda = 100$ and $\gamma = 0$ for Some Values of τ_m

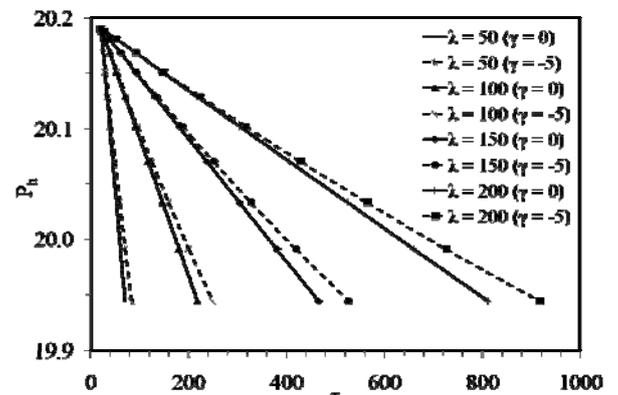


Fig 4: Compressive Load Beyond Bifurcation of Rod as a Function of Temperature Rise for Some Prescribed Values of λ

The characteristics curves showing the load-temperature relationship in case of uniform heating ($\tau_d = 0$) is given in Fig. 4. These curves are all

monotonously decreasing function of dimensionless temperature rising. Once the critical buckling load is reached and temperature is progressively increased, the compressive axial force arising in the boundaries falls considerably. In fact, the nature of these curves qualitatively analogous with the experimental findings of the works of Correia Rodrigues et al. [15].

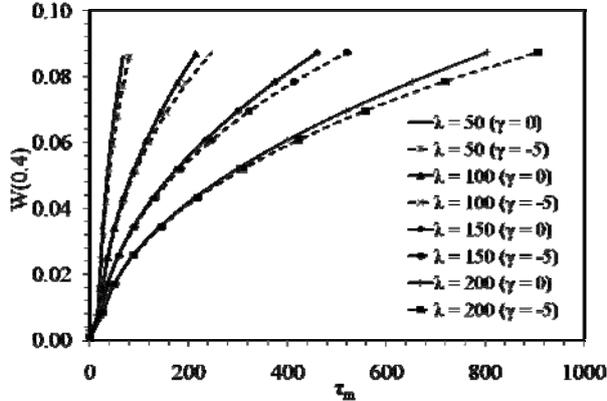


Fig 5: Maximum Deflection of Bar as a Function of Temperature Rise τ_m with $\tau_d = 10$ for Some Prescribed Values of λ

4.4 Effect of Slenderness Ratio

In order to illustrate the influence of the slenderness parameter λ on the buckling deformation, the secondary equilibrium paths of the thermally postbuckled bar subjected to a non-uniform temperature rising ($\tau_d = 10$) with different values of λ in terms of maximum deflection $W(0.4)$ versus τ_m is plotted in Fig. 5. Due to the effect of non-uniform heating, the intersection points of the curves with the coordinate τ_m axis are not the same and the value is just below the critical temperature parameter τ_{cr} . When $\tau_m > \tau_{cr}$, the postbuckling deformations are totally dependent on λ , which is a feature of nonlinear theory of the bar with axial extension. It is definitely noteworthy from Fig. 5 that an increase of slenderness ratio from 100 to 200 possesses the same deformed secondary equilibrium path of the pinned-fixed bar but at higher mean temperature rise. On the other hand, for a particular non-dimensional temperature rise, the maximum deflection of the bars increases stridently with the decrease of the bar slenderness ratios.

4.5 Effect of nonlinear thermal strain coefficient

In this paper, extensive analyses are carried out to control the thermal buckling of a bar made of a physically nonlinear thermo-elastic material as proposed by Smith et al. [14]. Here γ , used throughout this study, represents a coefficient that expresses nonlinear characteristics of a material. The coefficient $\gamma = -5$ is relatively large for steels, but it is assumed to emphasize nonlinear effects. A safe buckling temperature for a linear case is smaller than the corresponding nonlinear one when the coefficient γ is negative (Fig. 5). Furthermore, the growth of the postbuckling deflections is more rapidly developed with the introduction of nonlinear strain temperature coefficient. These effects have similar nature in all the characteristics curves compared with the linear cases. However, more

dominant rise of nondimensional temperature with the governing parameters is observed for very high slenderness ratios.

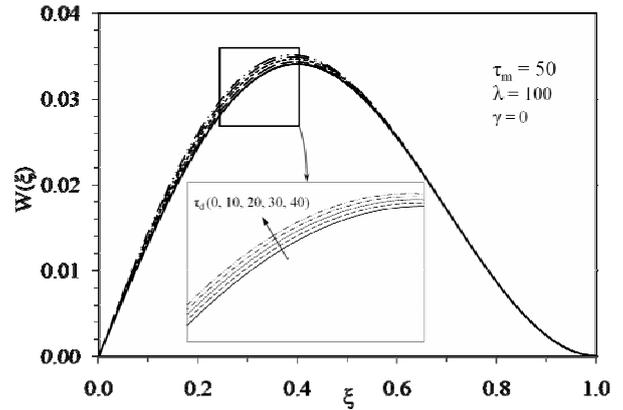


Fig 6: Thermal Post-Buckling Configuration of Bar with $\tau_m = 50$, $\lambda = 100$ and $\gamma = 0$ for Some Values of τ_d

4.6 Effect of transverse temperature rise

For some prescribed values of transverse temperature rise parameter τ_d , the postbuckling equilibrium configuration is shown in Fig. 6. For a comparison, the secondary equilibrium paths of the bars with $\tau_d = 0$ is also plotted in solid line. From these curves, it is found that the bending deformation produced by transverse temperature change τ_d is the main part in the whole deformations when the mean temperature rising parameter $\tau_m < \tau_{cr}$. For pinned end, an outstanding dominance on τ_d on the postbuckling deformation of the bar is clearly distinguished from the fixed end condition. The reason behind this occurrence can be explained by the kinematic conditions of pinned-fixed bar as described in Eqs. (9)-(10).

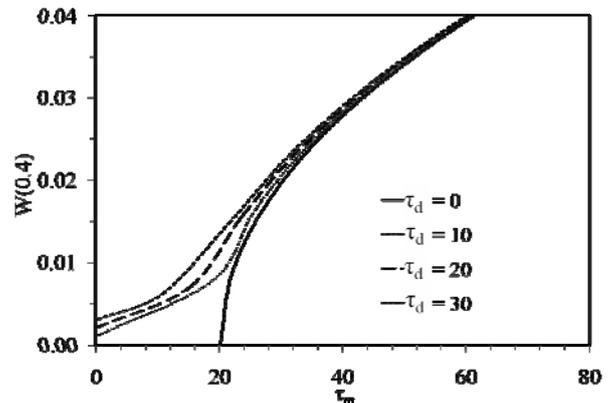


Fig 7: Thermal Post-Buckling Equilibrium Paths $W(0.4) - \tau_m$ of Bar with $\lambda = 100$ and $\gamma = 0$ for Some Values of τ_d

From the characteristics curves of maximum deflection versus τ_m as shown in Fig. 7, it is clear that the dominance of τ_d on maximum deflection is also varied for different τ_m . When $\tau_m < \tau_{cr}$, the bending deformation produced by τ_d significantly increases the maximum deflection. But, when $\tau_m > \tau_{cr}$, the contribution of axially thermal expansion to the transverse deformation becomes more and more significant with the increment of the mean temperature rise τ_m .

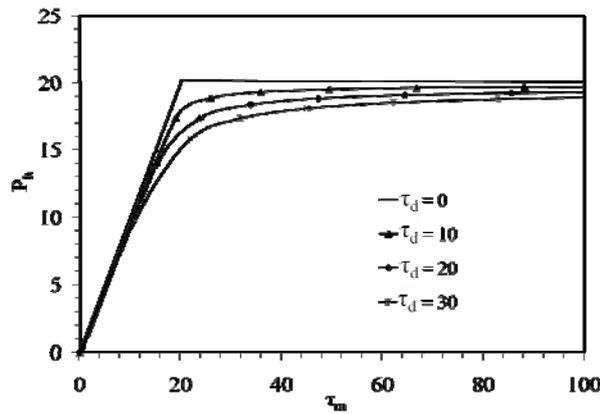


Fig 8: Thermal Post-Buckling Equilibrium Paths $P_h - \tau_m$ of Bar with $\lambda = 100$ and $\gamma = 0$ for Some Values of τ_d

The relations between the dimensionless horizontal constrained force, P_h and the mean temperature rise parameter, τ_m for different values of τ_d are given in Fig. 8. The curves with large τ_d , hence a higher thermal moment, bend over more than those with small τ_d . Also, as τ_d approaches zero, the curves approach the behavior of an axially restrained rod with only τ_m , i.e. a bifurcation on thermal buckling problem with no transverse deflection until the critical temperature has been reached. All curves also asymptotically approach $(P_h)_{cr}$ as the τ_m goes to infinity.

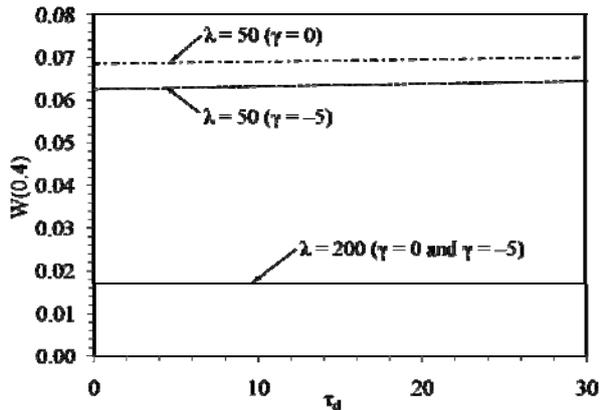


Fig 9: Maximum Deflection of Pinned-Fixed Bar as a Function of Temperature Rise τ_d with $\tau_m = 50$ for Some Prescribed Values of λ and γ

Figure 9 show the effect of nonlinear strain-temperature coefficient on the maximum deflection with the variation of transverse temperature rise parameter. These curves make a reverse performance as described earlier and negligible increase of maximum deflection can only be found with the increase of transverse temperature rise at lower slenderness ratio.

5. CONCLUSIONS

This paper has presented the results of a numerical study of the postbuckling behavior of a slender elastic bar with pinned-fixed end subjected to non-uniform heating. In particular, this study has focused on how the end constrained of the bar structure affects the postbuckled deformation under non-uniform transverse temperature rise. From the results of this study, the following conclusions may be drawn.

(1) Due to non-uniform heating, both thermal expansion and thermal bowing induce buckling in the structure. The postbuckling analysis of slender elastic bars subjected to both uniform and non-uniform temperature variation is highly dependent on the prescribed end conditions.

(2) The nonlinear strain-temperature coefficient shows a remarkable influence on the critical buckling temperature and postbuckling response of the heated bar. The nonlinearity effects become significant with the increase of the slenderness for uniform mean temperature rise variation but reverse trend is observed for non-uniform transverse temperature rise variation.

(3) The thermal post-buckling of a bar develops slowly and monotonously along with increase of the mean temperature rise. The dimensionless buckling parameters are also sensitive to the slenderness ratio of the bar and show the consistent behavior for both uniform and non-uniform heating conditions.

(4) The equilibrium path of the non-uniformly heated bar is similar to that of an initially deformed beam because of the thermal bending moment produced in the bar by the transverse change.

(5) The pinned end is more sensible to transverse temperature rise than the fixed end and hence the fixed ended bar renders more safety at higher temperature with minimum deflection.

(6) It is observed that the bar having higher slenderness ratio gives lower maximum deflection at the same mean temperature rise.

6. REFERENCES

1. El Naschie, M. S., 1976, "Thermal Initial Post-Buckling of the Extensional Elastica", *Int. J. Mech. Sci.*, 18:321-324.
2. Li, S. R., 2000, "A Shooting Method for Thermal Post-Buckling of Rods with Pinned-Fixed Ends", *Journal of Gansu University of Technology*, 4:106-110.
3. Li, S. R., 2000, "Thermal Post-Buckling of Asymmetrically Supported Elastic Rods", *Engineering Mechanics*, 17(5):115-119.
4. Li, S. R., and Cheng, C. J., 2000, "Analysis of Thermal Post-Buckling of Heated Elastic Rods", *Appl. Math. Mech. (English ed.)*, 21(2):133-140.
5. Li, S. R., and Zhou, Y.-H., 2001, "Thermal Post-Buckling of Rods with Variable Cross Sections", *Proc. 4th International Congress on Thermal Stresses*, pp. 147-150.
6. Li, S. R., Zhou, Y.-H., and Zheng, X., 2002, "Thermal Post-Buckling of a Heated Elastic Rod with Pinned-Fixed Ends", *J. Thermal Stresses*, 25:45-56.
7. Li, S. R., Cheng, C. J., and Zhou, Y.H., 2003, "Thermal Post-Buckling of an Elastic Beams Subjected to a Transversely Non-Uniform Temperature Rising", *Appl. Math. Mech. (English ed.)*, 24(5):514-520.
8. Vaz, M. A., and Solano, R. F., 2003, "Post-Buckling Analysis of Slender Elastic Rod Subjected to Uniform Thermal Loads", *J. Thermal Stresses*, 26:847-860.

9. Vaz, M. A., and Solano, R. F., 2004, "Thermal Post-Buckling of Slender Elastic Rods with Hinged Ends Constrained by a Linear Spring", J. Thermal Stresses, 27:367–380.
10. Saha, S., 2007, "Post Buckling Analysis of a Slender Bar under Transversely Non-Uniform Temperature Rise", M.Sc. Engg. thesis, Bangladesh University of Engineering and Technology, Dhaka, Bangladesh.
11. Kalnins, A. and Lestingi, J.F., 1967, "On Nonlinear Analysis of Elastic Shells of Revolution", J. Appl. Mech., Ser. E, 34(1):59-64.
12. Sepetoski, W.K., Pearson, C.E., Dingwell, I.W., and Adkins, A.W., 1962, "A Digital Computer Program for the General Axially Symmetric Thin Shell Problem", J. Applied Mech., Ser. E., 29:655-661.
13. Mathcad, 2006, Mathcad 14 Professional for PC, Mathsoft Inc.
14. Smith, R.T., Stern, R., and Stephens, P.W., 1966, "Third Order Elastic Moduli of Polycrystalline Metals from Ultrasonic Measurements", J. Acoust. Soc. Amer., 40:1002–1008.
15. Correia Rodrigues, J.P., Cbrita Neves, I., and Valente, J.C., 2000, "Experimental Research on the Critical Temperature of Compressed Steel Elements with Restrained Thermal Elongation", Fire Safety Journal, 35:77–98.

7. NOMENCLATURE

Symbol	Meaning	Unit
A	Cross-sectional area of the structure	m^2
b	width of the bar cross-section	m
ds	deformed length	m
E	Young's modulus of elasticity	N/m^2
h	height of the bar cross-section	m
H	Horizontal resultant Compressive force	N
I	cross-sectional second moment of inertia	m^4
k	Uniform curvature	m^{-1}
K	Nondimensional curvature	
L	undeformed length of the bar	m
L_o	Constants related to material nonlinearity with temperature	$N.m^{-2}$
m	Non-dimensional bending moment	
M	Bending moment	$N.m$
P_h	Non-dimensional horizontal resultant Compressive force	
P_v	Non-dimensional vertical resultant force	
s	Neutral axis of the deformed bar	m
S	Non-dimensional arc length of the deformed neutral axis	
T	Temperature rise	$^{\circ}C$
T_d	Temperature change from one surface to other in y-direction	$^{\circ}C$
T_m	Average bar temperature rise	$^{\circ}C$
T^+	Non-uniform transverse temperature rise at top surface	$^{\circ}C$

T^-	Non-uniform transverse temperature rise at bottom surface	$^{\circ}C$
u	horizontal displacement of the undeformed element	m
U	Non-dimensional horizontal displacement	
V	Vertical resultant force	N
w	vertical displacement of the undeformed element	m
W	Non-dimensional vertical displacement	
x, y, z	Cartesian coordinates	m
Greek Symbols		
α	Thermal expansion coefficient	$/^{\circ}C$
θ	rotational angle of the cross-section	$^{\circ}$
θ_o	End rotational Angle	$^{\circ}$
γ	Nonlinear strain-temperature coefficient	
λ	Slenderness ratio	
μ	Stretching ratio	
ξ	Non-dimensional length of undeformed neutral axis	
π	Pi number	
τ_m	Non-dimensional mean temperature rise	
τ_d	Non-dimensional transverse temperature rise	
Subscript		
c	Compressive	
cr	Critical	
o	End point	